Organometallics **1994,** *13,* 2391–2396

Transition Metal Chemistry of Main Group Hydrazides. 8.[1] A New Long-Chain Diphosphine with the P^{III}–N–N–P^{V}–N–N–P^{III} Backbone as a Chelating Ligand for Molybdenum, Platinum, and Palladium. Crystal and Molecular Structures of *cis*-$[Mo(CO)_4\{PhP(S)[N(Me)NHP(i\text{-}Pr)_2]_2\}]$ and *cis*-$[PtCl_2\{PhP(S)[N(Me)NHP(i\text{-}Pr)_2]_2\}]$

V. Sreenivasa Reddy,† Kattesh V. Katti,*,† and Charles L. Barnes‡

Center for Radiological Research and MU Research Reactor, Allton Building Laboratories,
301 Business Loop 70 West, Columbia, Missouri 65203, and Department of Chemistry,
University of Missouri, Columbia, Missouri 65211

Received December 13, 1993⊗

The reaction of $PhP(S)[N(Me)NH_2]_2$ (**1**) with $(i\text{-}Pr)_2PCl$ gave the new long-chain diphosphine ligand $PhP(S)[N(Me)NHP(i\text{-}Pr)_2]_2$ (**2**) in good yields. The reactions of the new ligand **2** with $[Mo(CO)_4(NHC_5H_{10})_2]$, $PtCl_2(COD)$, and $PdCl_2(PhCN)_2$ gave the eight-membered metallacyclic compounds *cis*-$[Mo(CO)_4\{PhP(S)[N(Me)NHP(i\text{-}Pr)_2]_2\}]$ (**3**), *cis*-$[PtCl_2\{PhP(S)[N(Me)NHP(i\text{-}Pr)_2]_2\}]$ (**4**), and *cis*-$[PdCl_2\{PhP(S)[N(Me)NHP(i\text{-}Pr)_2]_2\}]$ (**5**) in good yields. The X-ray crystal structures of **3** and **4** have been determined; (**3**) monoclinic, space group $P2_1/n$, with $a = 8.555(2)$ Å, $b = 19.045(2)$ Å, $c = 19.700(3)$ Å, $\beta = 98.59(1)°$, $Z = 4$, and $R = 0.028$; (**4**) monoclinic, space group $P2_1/c$, with $a = 10.608(2)$ Å, $b = 18.714(2)$ Å, $c = 15.404(4)$ Å, $\beta = 109.41(1)°$, $Z = 4$, and $R = 0.037$.

Introduction

The transition metal chemistry of chelating phosphine ligands has been the subject of extensive research because of their role in metal mediated homogeneous catalysis.[2-5] Several studies have shown that the size of the chelate ring exerts a dramatic influence on the reactivity and the catalytic activity of the metal complex. For example, recent studies by Milstein have shown that reducing or increasing the size of the diphosphine chelating ligand by one carbon unit (*e.g.* $R_2P(CH_2)_nPR_2$; $n = 2$, 3, or 4) results in a substantial change in the catalytic activity of the corresponding Pd(0) complexes.[6-8] The importance of the diphosphine chain length on the overall reactivity and catalytic activity of the Rh(I) complexes has also been conclusively demonstrated by Wegman and others in the catalytic reductive carbonylation of methanol.[9-11] Their studies have revealed that selectivities greater than 80% can be achieved with diphosphines of the type $R_2P(CH_2)_3PR_2$. However, shortening or lengthening the diphosphine bridge resulted in substantial loss in catalytic activity. Although there are no generalizations on the exact size of the alkane diphosphine ($R_2P(CH_2)_nPR_2$) chain lengths to be used in the design of efficient catalysts, there is, however, some consensus that the diphosphine ligands which form highly stable metal chelates generally exhibit diminished reactivity and catalytic activity.[6-11] For the aforementioned reasons, there is renewed interest in the main group and transition metal chemistry of diphosphine ligands of long chain lengths which provide chelate interactions with metal centers. In this context, we reasoned that the phosphorus dihydrazides of the type $H_2NN(Me)P(E)N(Me)NH_2$ can be used as building blocks to construct new long-chain diphosphines upon their interaction with the appropriate phosphorus halides. For example, the phosphorus hydrazido diphosphine ligands (**A**) will have five

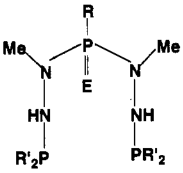

(A)

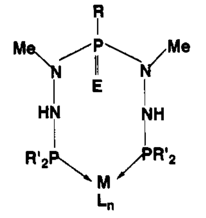

(B)

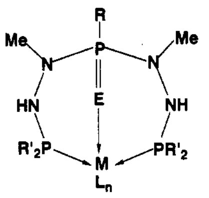

(C)

atoms (i.e., –N–N–P–N–N–) bridging the phosphine units and, therefore, may compare (or contrast) with the five carbon bridging alkane diphosphines of the type $R_2P(CH_2)_5PR_2$. Given these facts, two questions are of special interest. First, what would be the mode of

---

* To whom correspondence should be addressed.

† Center for Radiological Research and MU Research Reactor.

‡ Department of Chemistry.

⊗ Abstract published in *Advance ACS Abstracts,* May 1, 1994.

[1] Part 7: Reddy, V. S.; Katti, K. V. *Inorg. Chem.*, in press.

[2] Parshall, G. W. *Homogeneous Catalysis*; Wiley; New York, 1980.

[3] Pignolet, L. H., Ed. *Homogeneous Catalysis with Metal Phosphine Complexes*; Plenum: New York, 1983.

[4] Alper, H.; Saldana-Maldonado, M.; Lin, I. J. B. *J. Mol. Catal.* **1988,** *49,* L27.

[5] Pisano, C.; Mezzett, A.; Consiglio, G. *Organometallics* **1992,** *11,* 20.

[6] Portnoy, M.; Milstein, D. *Organometallics* **1993,** *12,* 1655.

[7] Portnoy, M.; Milstein, D. *Organometallics* **1993,** *12,* 1665.

[8] David, B. Y.; Gozin, M.; Portnoy, M.; Milstein, D. J. *J. Mol. Catal.* **1992,** *73,* 173.

[9] Hoyashi, T.; Kawabata, Y.; Isoyama, T.; Ogata, I. *Bull. Chem. Soc. Jpn.* **1981,** *54,* 3438.

[10] (a) Wegman, R. W.; Miller, D. S. U.S. Pat. 4 594 463, 1986. (b) Wegman, W.; Moloy, K. G. U. S. Pat. 4 727 200, 1988. (c) Moloy, K. G.; Wegman, R. W. *J. Chem. Soc., Chem. Commun.* **1988,** 820. (d) Moloy, K. G.; Wegman, R. W. *Organometallics* **1989,** *8,* 2883.

[11] Morteux, A.; Petit, F. In *Homogeneous Transition Metal Catalyzed Reactions*; Moser, W. R., Slocum, D. W., Eds.; Advances in Chemistry Series 230; American Chemical Society: Washington, DC, 1992; Chapter 18.

0276-7333/94/2313-2391$04.50/0

coordination (chelate vs nonchelate) of these new ligands (**A**) with the transition metals? And second, what influence will the bridging functionalities, such as N or P(S), in **A** have on the overall chelate effect? Specifically, will the bridging unit in **A** interact with the metal center to destroy the eight-membered metal chelate **B** to produce six-membered bicyclic smaller chelates (**C**)? These questions are relevant in the design of large diphosphine metal chelates which tend to be less stable (and catalytically more active), while the smaller sized chelates (five- or six-membered) are, generally, very stable and exhibit diminished catalytic reactivity. As part of our ongoing studies on the transition metal chemistry of chelating phosphines and phosphorus hydrazides,[12-17] we describe the synthesis of a new class of diphosphine ligands of the type A. The application of this new ligand system in the design of eight-membered chelate rings of Mo(0), Pd(II), and Pt(II) is also described.

Results and Discussion

Ligand Synthesis. The precursor phosphorus hydrazide, **1**, is readily produced in good yield by the reaction of $PhP(S)Cl_2$ with a 6–8-fold excess of methylhydrazine. The choice of an *N*-methyl substituent α to the central phosphorus, rather than N–H, was based on the reasoning to direct the incoming phosphine units at the terminal hydrazido nitrogens, as depicted in eq 1. The phosphorus hydrazido bridged new diphosphine, $PhP(S)[N(Me)NHP(i\text{-}Pr_2)]_2$ (**2**), was prepared by the nucleophilic substitution reaction of the phosphorus hydrazide $PhP(S)[N(Me)NH_2)]_2$ (**1**) with $(i\text{-}Pr)_2PCl$ (eq 1). The new ligand **2**, is an air-stable viscous oil, and its chemical composition was established by C, H, and N analytical data. The P^{III}, P^{V} construction of **1** was evident from the AX_2 spin pattern in its ^{31}P NMR spectrum. The triplet centered at 87.3 ppm ($^3J(P-P)$ = 13.5 Hz), attributed to the P(S) functionality, indicates a modest deshielding compared to its precursor ($\delta(^{31}P)$ for **1** = 86.5). The two phosphine units in **2** resonate as a doublet centered at 68.3 ppm ($^3J(P-P)$ = 13.5 Hz), and this chemical shift is consistent with the trivalent phosphorus functionality.

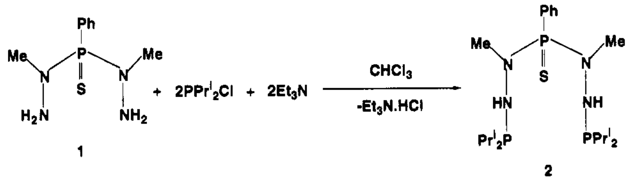

(1)

Coordination Chemistry of 2. The presence of two trivalent phosphorus centers, and their mutual disposition across the N–N–P^V–N–N skeleton in **2**, presents the possibility of using them as chelating π-acid donors toward transition metals. For example, **2** reacted smoothly with *cis*-$[Mo(CO)_4(NHC_5H_{10})_2]$ in dichloromethane to produce the new metallacyclic compound **3**, in good yields (Scheme 1). The chemical composition of **3** was confirmed by C, H, and N analysis. The ^{31}P NMR spectrum of **3** consisted of an AX_2 spin pattern with a doublet (attributed to $P(i\text{-}Pr)_2$ groups) and triplet (attributed to the P(S) functionality) centered at 112.8 and 97.1 ppm, respectively. The equivalence of the $P(i\text{-}Pr)_2$ centers, as evidenced by the ^{31}P NMR spectrum, supports the chelate structure with a *cis* disposition of the phosphine units around the metal center. A 25 ppm deshielding in the ^{31}P NMR chemical shifts of the phosphine functionalities on going from the free ligand **2** to the Mo(0) complex **3** is consistent with the coordination of a zerovalent early transition metal with the phosphine units. However, the P(S) functionality in **3**, which resonated at 97.1 ppm, signifies a considerable deshielding (~10 ppm) compared to the free ligand **2** (87.3 ppm) despite the fact that the Mo(0) is four bonds away from this phosphine sulfide (P(S)) center. In order to confirm that **3** is a large eight-membered chelate rather than a bicyclic framework (as depicted in **C**), an X-ray crystallographic analysis of this compound has been carried out. The ORTEP plot shown in Figure 1 confirms that the structure of **2** comprises the neutral monomeric eight-membered chelate of Mo(0). Selected bond distances and angles for **2** are summarized in Table 1. The most notable aspect is the lack of an interaction between the phosphorus chalcogenide (P(S)) and the metal center. The complex shown in Figure 1 contains Mo(0) in a distorted octahedral geometry with the $[PhP(S)\{N(Me)NHP(i\text{-}Pr)_2\}_2]$ chelating in a *cis* fashion via the two phosphine groups. The *cis* disposition of the carbonyl groups as indicated by the IR spectrum of **3** is seen in its structure. The metal carbonyl distances Mo–C1 (1.976(4) Å) and Mo–C3 (1.975(4) Å) are shorter compared to Mo–C2 (2.032(4) Å) and Mo–C4 (2.027(4) Å). In addition, the C–O distances corresponding to the Mo–C1 (C1–O1 = 1.152(4) Å) and Mo–C3 (C3–O3

Scheme 1

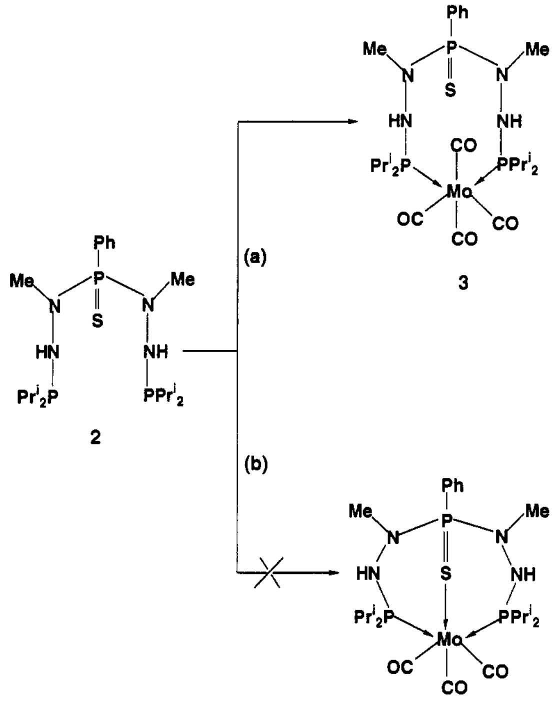

(a) = *cis*-$[Mo(CO)_4(NHC_5H_{10})_2]$ or *fac*-$[Mo(CO)_3(CHT)]$

(b) = *fac*-$[Mo(CO)_3(CHT)]$

---

(12) Katti, K. V.; Barnes, C. L. *Inorg. Chem.* **1992**, *31*, 4231.

(13) Singh, P. R.; Jimenez, H.; Katti, K. V.; Volkert, W. A.; Barnes, C. L. *Inorg. Chem.* **1994**, *33*, 736.

(14) Katti, K. V.; Singh, P. R.; Barnes, C. L. *Inorg. Chem.* **1992**, *31*, 4588.

(15) Wang, M. W.; Volkert, E. W.; Singh, P. R.; Katti, K. K.; Lusaik, P.; Katti, K. V.; Barnes, C. L. *Inorg. Chem.* **1994**, *33*, 1184.

(16) Katti, K. V.; Ge, Y. W.; Singh, P. R.; Date, S. V.; Barnes, C. L. *Organometallics* **1994**, *13*, 541.

(17) Katti, K. V.; Singh, P. R. Unpublished results.

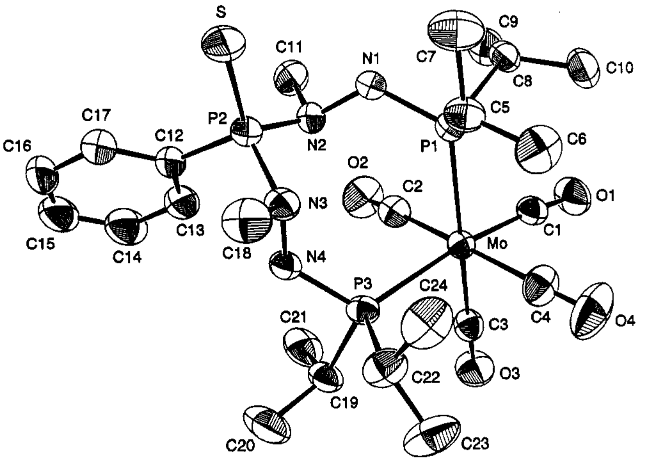

Figure 1. ORTEP representation of structure 3. The thermal ellipsoids are drawn at the 50% probability level.

Table 1. Selected Bond Lengths (Å) and Angles (deg) for Compound 3

Mo–P1	2.567(1)	Mo–P3	2.567(1)
Mo–C1	1.976(4)	Mo–C2	2.032(4)
Mo–C3	1.976(4)	Mo–C4	2.029(4)
C1–O1	1.152(4)	C2–O2	1.144(5)
C3–O3	1.152(4)	C4–O4	1.141(5)
P1–N1	1.695(3)	P1–C5	1.868(3)
P1–C8	1.857(3)	P2–S	1.937(2)
P2–N2	1.693(3)	P2–N3	1.701(3)
P2–C12	1.807(3)	P3–N4	1.711(3)
P3–C19	1.868(3)	P3–C22	1.865(4)
N1–N2	1.424(4)	N2–C11	1.473(4)
N3–N4	1.429(4)	N3–C18	1.486(4)

P1–Mo–P2	97.0(1)	P1–Mo–C1	91.6(1)
P1–Mo–C2	88.8(1)	P1–Mo–C3	175.7(1)
P1–Mo–C4	97.3(1)	P3–Mo–C1	171.4(1)
P3–Mo–C2	90.4(1)	P3–Mo–C3	85.9(1)
P3–Mo–C4	95.3(1)	C1–Mo–C2	89.7(1)
C1–Mo–C3	85.5(1)	C1–Mo–C4	83.6(2)
C2–Mo–C3	88.0(1)	C2–Mo–C4	171.1(1)
C3–Mo–C4	85.5(1)	Mo–P1–N1	115.3(1)
Mo–P1–C5	120.5(1)	Mo–P1–C8	116.2(1)
N1–P1–C5	101.2(2)	N1–P1–C8	97.0(1)
C5–P1–C8	103.0(2)	S–P2–N2	114.1(1)
S–P2–N3	112.4(1)	S–P2–C12	114.0(1)
N2–P2–N3	101.8(1)	N2–P2–C12	114.0(1)
N3–P2–C12	105.8(2)	Mo–P3–N4	118.7(1)
Mo–P3–C19	112.6(1)	Mo–P3–C22	117.7(1)
N4–P3–C19	97.4(1)	N4–P3–C22	106.6(2)
C19–P3–C22	100.6(2)	P1–N1–N2	125.8(2)
P2–N2–N1	109.8(2)	P2–N2–C11	116.4(2)
N1–N2–C11	108.6(2)	P2–N3–N4	111.3(2)
P2–N3–C18	115.9(2)	N4–N3–C18	112.9(3)
P3–N4–N3	120.9(2)	Mo–C1–O1	174.9(3)
Mo–C2–O2	173.1(3)	Mo–C3–O3	177.0(3)
Mo–C4–O4	170.0(3)		

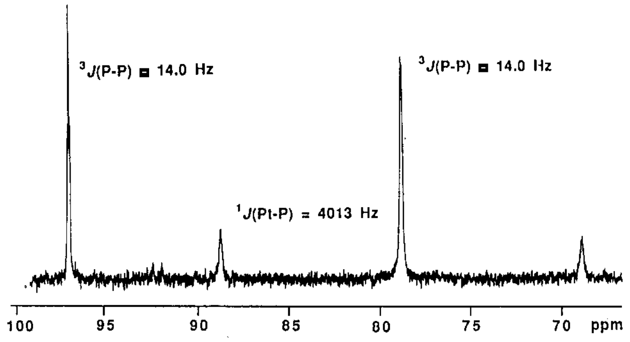

Figure 2. ^{31}P NMR (202.5-MHz) spectrum of *cis*-[PtCl$_2${PhP(S)[N(Me)NHP(*i*-Pr)$_2$]$_2$}] (4).

Scheme 2

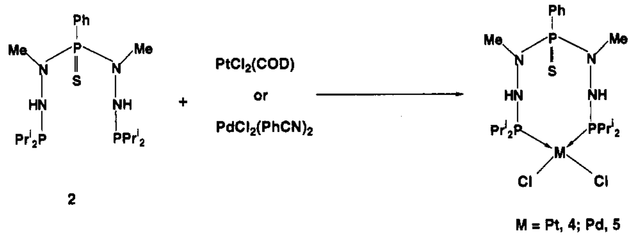

= 1.152(4) Å) groups are longer compared to the C–O distances of the Mo–C2 and Mo–C4 carbonyls. The carbonyl groups C3–O3 and C1–O1 are *trans* to the P1 and P3 phosphines, respectively, whereas C4–O4 and C2–O2 are disposed *trans* to each other across the metal center. The differences in the two sets of Mo–C–O distances [i.e., C3–O3 and C1–O1 vs C4–O4 and C2–O2] as discussed above are consistent with the poor π-accepting capability of the phosphines as compared to the carbonyl groups. The Mo–P distances in 3 (Mo–P1 = 2.567(9) Å, Mo–P2 = 2.567(9) Å) appear to be longer compared to those found in many phosphine complexes of Mo(0) and W(0).[18] This may, presumably, be due to the localization of electronic charge within the P^V–N–N–P^{III} framework rather than in the P^V–N–N–P^{III}–Mo bonds of 3. This is consistent with the shorter N–N distances in 3 (N1–N2 = 1.424(4) Å; N3–N4 = 1.424(4) Å) as compared to those in the uncoordinated free ligand 1.

Interestingly, the geometry around N2 and N3 is trigonal pyramidal rather than trigonal planar. The P(S) functionalities of phosphorus hydrazides have shown propensity to coordinate with both the early and late transition metals.[13-17] However, the lack of such an interaction in 3 may be due to electronic rather than steric effects. The N–P–N angle (101.8°) in 3 is sufficiently wide for P=S to interact with Mo. A repulsive interaction between the sulfur and C–O [C2–O2 or C4–O4] groups may also contribute to the lack of P(S) coordination with the metal center. We have also reasoned that the third carbonyl group from 3 should be readily displaced before Mo can coordinate with the sulfur of the phosphorus chalcogenide. Therefore, we have investigated the reaction of 2 with *fac*-[Mo(CO)$_3$(CHT)] (CHT = cycloheptatriene), which has three easily replaceable ligands on Mo (Scheme 1). The formation of 3 exclusively from this reaction demonstrates the unique ability of the new diphosphine ligand 2 to produce large eight-membered chelates. Similar reactions involving the disproportionation of M(CO)$_3$L$_3$ to M(CO)$_4$L$_2$ are known for molybdenum and tungsten precursors.[19] We have also investigated the efficacy of 2 to produce metal complexes with the electron-rich late transition metals, as outlined below.

The new diphosphine 2 also reacts efficiently with PtCl$_2$(COD) and PdCl$_2$(PhCN)$_2$ in dichloromethane to produce the metallacyclic compounds of Pt(II) and Pd(II), respectively, [PhP(S){N(Me)NHP(*i*-Pr)$_2$}$_2$MCl$_2$] (M = Pt (4), Pd (5)), in near quantitative yield (Scheme 2). Their composition was established by C, H, and N analytical and multinuclear NMR spectroscopic data. The ^{31}P NMR spectra of 4 (Figure 2) and 5 consisted of features of an AX$_2$ spin system with the triplets (centered at 97.0 ppm

---

[18] Reddy, V. S.; Krishnamurthy, S. S.; Nethaji, M. *J. Organomet. Chem.* **1992**, *438*, 99 and references therein.

[19] King, R. B.; Korenowski, T. F. *Inorg. Chem.* **1971**, *10*, 1188.

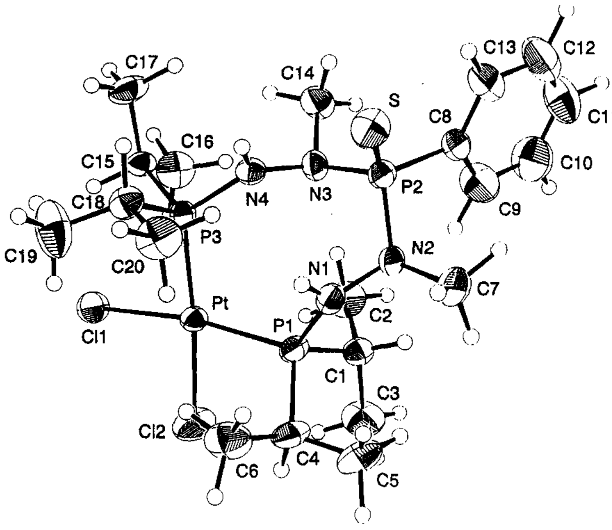

Figure 3. ORTEP representation of structure 4. The thermal ellipsoids are drawn at the 50% probability level.

(^3J(P–P) = 14.0 Hz) for 4 and 97.0 ppm (^3J(P–P) = 12.5 Hz) for 5) and doublets (centered at 78.8 ppm (^3J(P–P) = 14.0 Hz) for 4 and 110.7 ppm (^3J(P–P) = 12.5 Hz) for 5) attributed to the P(S) and P(i-Pr)$_2$ groups, respectively. The observation of a large ^1J(Pt–P) value of 4013 Hz was diagnostic of the two phosphines involved in the coordination with the metal to produce the metallacycle 4. The large ^1J(Pt–P) value also suggests that the phosphine groups may be *trans* to the polarizable chloride substituents. The remarkable upfield (more negative) ^{31}P chemical shift for the P(i-Pr)$_2$ groups on going from the palladium to the platinum complexes [(i-Pr)$_2$P(Pd) = 110.7 ppm; P(i-Pr)$_2$P(Pt) = 78.8 ppm] may be rationalized in terms of a somewhat stronger M–P bonding interaction in the platinum complex than in the palladium analogue.

In order to gain further insight into the bonding features of 2 with the late transition metals and also to find out if P(S) or any additional heteroatoms of 2 interact with the metal, a single crystal X-ray diffraction analysis of the platinum complex 4, as a representative, has been carried out. The ORTEP drawing shown in Figure 3 reveals that the structure of 4 comprises the neutral monomeric complex [PhP(S){N(Me)NHP(i-Pr)$_2$}$_2$PtCl$_2$]. Selected bond distances and angles for non-hydrogen atoms are listed in Table 2. The complex, shown in Figure 3, contains Pt in a typical square planar environment with the two phosphine units of 2 chelating in an eight-membered metallacycle via a *cis* disposition of the phosphines. The geometry around N2 and N3 in 4 is trigonal pyramidal with the angles adding to 340.2(4) and 333.7(5)°, respectively.

Conformation of the Eight-Membered Metallacycles 3 and 4. The crystallographic data for the Mo(0) and Pt(II) metallacyclic compounds suggest that the eight-membered rings are nonplanar. The stereoview of the Mo(0) complex 3 indicates that the eight-membered ring has a twisted chair conformation. The stereoview of the Pt(II) complex, 4, indicates it to be in a crown conformation. The influence of the phosphorus substituents on the coordination chemistry of 1 and its derivatives has been well established.[16,17] For example, alkyl or aryl substituents on the phosphorus in 1 favored N–S coordination with the transition metal centers via five-membered metallacycles.[16] However, the introduction of oxygen-containing substituents on the phosphorus (e.g. alkoxy or aryloxy), presumably makes the sulfur in 1 and related derivatives less nucleophilic and hence results in the six-membered metallacyclic compounds via the coordination of the two terminal hydrazine units with no interactions with the sulfur center.[16,17] Studies to investigate the effect of substituents on the phosphorus and nitrogen on the overall conformation of the eight-membered rings of the type 3–5 are underway.

Table 2. Selected Bond Lengths (Å) and Angles (deg) for Compound 4

Pt–Cl1	2.361(2)	Pt–Cl2	2.350(2)
Pt–P1	2.235(2)	Pt–P3	2.260(2)
P1–N1	1.674(7)	P1–C1	1.850(8)
P1–C4	1.833(9)	P2–S	1.941(3)
P2–N2	1.685(6)	P2–N3	1.714(6)
P2–C8	1.811(8)	P3–N4	1.687(6)
P3–C15	1.840(7)	P3–C18	1.849(8)
N1–N2	1.423(9)	N2–C7	1.483(10)
N3–N4	1.436(8)	N3–C14	1.490(10)
Cl1–Pt–Cl2	84.6(1)	Cl1–Pt–P1	170.1(1)
Cl1–Pt–P3	89.4(1)	Cl2–Pt–P1	85.4(1)
Cl2–Pt–P3	174.0(1)	P1–Pt–P3	100.6(1)
Pt–P1–N1	118.4(2)	Pt–P1–C1	113.6(3)
Pt–P1–C4	111.5(3)	N1–P1–C1	102.7(3)
N1–P1–C4	101.6(4)	C1–P1–C4	107.8(4)
S–P2–N2	114.4(3)	S–P2–N3	114.7(2)
S–P2–C8	114.6(3)	N2–P2–P3	102.4(3)
N2–P2–C8	103.6(3)	N3–P2–C8	105.9(3)
Pt–P3–N4	120.4(2)	Pt–P3–C15	110.6(2)
Pt–P3–C18	114.8(3)	N4–P3–C15	109.6(3)
N4–P3–C18	103.7(3)	P1–N1–N2	122.8(5)
P2–N2–N1	114.4(4)	P2–N2–C7	114.3(5)
N1–N2–C7	111.5(6)	P2–N3–N4	108.7(4)
P2–N3–C14	113.7(5)	N4–N3–C14	111.3(7)
P3–N4–N3	125.4(5)		

Conclusions

The present investigation demonstrates the utility of a main group hydrazide backbone to produce a new long-chain diphosphine 2. The formation of 2 through a simple nucleophilic substitution reaction of PhP(S)(NMeNH$_2$)$_2$ (1) with (i-Pr)$_2$PCl is of note, particularly in the context of the relatively difficult synthetic routes being used to produce the alkane bridged long-chain diphosphines (*e.g.* R$_2$P(CH$_2$)$_n$PR$_2$, n = 4, 5). The tendency of 2 to form the eight-membered metallacyclic chelates of Mo(0), 3, Pt(II), 4, and Pd(II), 5, reflects the highly selective nature of this new diphosphine to produce larger chelates. As a consequence, the chemistry described herein provides a simple access to large metallacyclic compounds with potential catalytic applications. The reason for the lack of interaction of the highly coordinating N–N–P(S)–N–N units of 2 with the metals is yet unclear. However, this puts an emphasis on the subsequent utility of the phosphorus chalcogenide and hydrazine nitrogens for coordination with other metals.

Experimental Section

All reactions were carried out under purified nitrogen by standard Schlenk techniques. Solvents were purified and dried by standard methods and distilled under nitrogen prior to use. Reagents such as (i-Pr)$_2$PCl, [Mo(CO)$_4$(NHC$_5$H$_{10}$)$_2$], PtCl$_2$(COD), and PdCl$_2$(PhCN)$_2$ were purchased from Aldrich Chemical Co. and were used without further purification. Triethylamine was distilled over KOH and stored over molecular sieves under N$_2$. Phosphorus bis(methyl hydrazido) sulfide (BHPS) was prepared by the reaction of PhP(S)Cl$_2$ with methylhydrazine.[20]

Nuclear magnetic resonance spectra were recorded on a Bruker AMX-500 spectrometer using $CDCl_3$ as the solvent. The ^1H NMR chemical shifts are reported in ppm, downfield from external standard $SiMe_4$. The ^{31}P NMR spectra were recorded with 85% H_3PO_4 as an external standard, and positive chemical shifts lie downfield of the standard. Infrared spectra were recorded using Nujol mulls and KBr cells on a Mattson Galaxy 3000 spectrophotometer. Elemental analyses were performed by Oneida Research Services, Inc., New York.

PhP(S){N(Me)NHP(*i*-Pr)₂}₂ (2). A solution of $(i\text{-}Pr)_2PCl$ (7.30 g, 0.478 mol) in chloroform (50 mL) was added dropwise to a mixture of $PhP(S)[N(Me)NH_2]_2$ (5.0 g, 0.217 mol) and triethylamine (4.83 g, 0.478 mol) also in chloroform (50 mL), at 25 °C with constant stirring. The reaction mixture was heated under reflux for 36 h under a stream of dry nitrogen (reaction was incomplete even after 24 h; ^{31}P NMR). The solvent was removed *in vacuo* and the residue was extracted from hexane and filtered through a column (2- ×3-cm) of Florisil. Evaporation of the solvent and excess $(i\text{-}Pr)_2PCl$ and Et_3N in vacuo affords the compound 2 in 85% yield as a colorless viscous oil. Anal. Calcd for $C_{20}H_{41}N_4P_3S$: C, 51.9; H, 8.9; N, 12.1. Found: C, 52.3; H, 8.7; N, 12.3. ^1H NMR δ 0.80–1.10 (m, 24H, CH_3(Pr)), 1.55 (m, 4H, CH(Pr)), 2.97 (d, ^3J(P–H) = 11.1 Hz, NCH_3), 3.61 (br, NH), 7.2–8.4 (m, 5H, Ph). ^{31}P NMR: δ 68.3 (d, ^3J(P–P) = 13.5 Hz, P(*i*-Pr)₂), 87.3 (t, ^3J(P–P) = 13.5 Hz, P(S)).

***cis*-[Mo(CO)₄{PhP(S)[N(Me)NHP(*i*-Pr)₂]₂}] (3).** To a solution of *cis*-$[Mo(CO)_4(NHC_5H_{10})_2]$ (0.20 g, 0.529 mmol) in dichloromethane (25 mL) was added dropwise at 25 °C a solution of $PhP(S)[N(Me)NHP(i\text{-}Pr)_2]_2$ (0.25 g, 0.529 mmol) also in dichloromethane (25 mL). The reaction mixture was heated under reflux for 8 h before the solvent was removed in vacuo to obtain a yellow microcrystalline powder. This residue was extracted from a mixture of CH_2Cl_2/hexane (1:1 ratio), and the extracts (3 × 10 mL) were filtered through a column of silica gel (20 g). Evaporation of the solvent *in vacuo* gave the title complex 2 in 70% yield (0.25 g). Mp: 142 °C dec. Anal. Calcd for $C_{24}H_{41}N_4O_4P_3SMo$: C, 42.9; H, 6.2; N, 8.3. Found: C, 43.1; H, 6.0; N, 8.4. IR (Nujol) (ν_{CO}): 2010 (sh), 1910 (s), 1898 (s), 1863 (vs) cm⁻¹. ^1H NMR: δ 1.15–1.40 (m, 24H, CH_3(Pr)), 2.0–2.22 (br, 4H, CH(Pr)), 2.60 (br, 3H, NCH_3), 2.95 3.61 (br, 3H, NCH_3), 3.80 (br, 2H NH), 7.2–8.4 (m, 5H, Ph). ^{31}P NMR: δ 112.8 (d, ^3J(P–P) = 13.5 Hz, P(*i*-Pr)₂), 97.1 (t, ^3J(P–P) = 13.5 Hz, P(S)).

***cis*-[PtCl₂{PhP(S)[N(Me)NHP(*i*-Pr)₂]₂}] (4).** A solution of 1 (0.38 g, 0.806 mmol) in dichloromethane (25 mL) was added dropwise to a solution of $PtCl_2$(COD) (0.30 g, 0.806 mmol) also in dichloromethane (25 mL) at 25 °C. The reaction mixture was stirred for 2 h and filtered. The filtrate was concentrated to ~5 mL. Addition of hexane (30 mL) gave a precipitate, which was filtered and dried *in vacuo* to obtain the title compound 4 in 90% yield (0.53 g) as a creamy white powder. Mp: 135 °C. Anal. Calcd for $C_{20}H_{41}Cl_2N_4P_3SPt$: C, 33.0; H, 5.7; N, 7.7. Found: C, 33.2; H, 5.6; N, 7.6. ^1H NMR: δ 1.22–1.55 (m, 24H, CH_3(Pr)), 1.60 (m, 4H, CH(Pr)), 2.40 (d, ^3J(P–H) = 15 Hz, 6H, NCH_3), 3.70 (d, ^3J(P–H) = 19.6 Hz, 3H, NH), 7.5–8.0 (m, 5H, Ph). ^{31}P NMR: δ 78.8 (d, ^3J(P–P) = 14.0 Hz, ^1J(Pt–P) = 4013 Hz, P(Pt)), 97.0 (t, ^3J(P–P) = 14.0 Hz, P(S)).

***cis*-[PdCl₂{PhP(S)[N(Me)NHP(*i*-Pr)₂]₂}] (5).** A solution of 1 (0.34 g, 0.785 mmol) in dichloromethane (25 mL) was added dropwise to a solution of $PdCl_2(PhCN)_2$ (0.30 g, 0.785 mmol) also in dichloromethane (25 mL) at 25 °C. The reaction mixture was stirred for 2 h and worked up as described above for 4 to give the title compound 5 in 95% yield (0.48 g) as yellow powder. Mp: 205 °C. Anal. Calcd for $C_{20}H_{41}Cl_2N_4P_3SPd$: C, 37.6; H, 6.5; N, 8.8. Found: C, 37.8; H, 6.6; N, 9.0. ^1H NMR: δ 1.20–1.40 (m, 24H, CH_3(Pr)), 1.70 (m, 4H, CH(Pr)), 2.40 (d, ^3J(P–H) = 14.5 Hz, 6H, NCH_3), 3.70 (d, ^2J(P–H) = 22.0 Hz, 2H, NH), 7.4–8.0 (m, 5H, Ph). ^{31}P NMR: δ 97.0 (t, ^3J(P–P) = 12.5 Hz, P(S)). 110.7 (d, ^3J(P–P) = 12.5 Hz, P(Pd)).

Reaction of *fac*-[Mo(CO)₃(CHT)] with 1. A dichloromethane (25 mL) solution of 1 (0.32 g, 0.734 mmol) was added dropwise to a solution of *fac*-$[Mo(CO)_3(CHT)]$ (0.20 g, 0.734 mmol) also in dichloromethane (25 mL) at 25 °C. The reaction mixture was heated under reflux for 4 h, and the solvent was removed in vacuo. The residue was extracted from a mixture of CH_2Cl_2/hexane (1:1 ratio) and the extracts (3 × 10 mL) were filtered through a column of silica gel (5 × 2 cm). Evaporation of the solvent *in vacuo* gave the yellow viscous oil. This was redissolved in a mixture of CH_2Cl_2/hexane (1:3 ratio) and cooled at 0 °C to obtain the tetracarbonyl complex 2 as a yellow

Table 3. Crystal Data for Compounds 3 and 4

	3	4
formula	$C_{24}H_{41}N_4O_4P_3SMo$	$C_{20}H_{41}Cl_2N_4P_3SPt$
cryst syst	monoclinic	monoclinic
space group	$P2_1/n$	$P2_1/c$
fw	670.53	728.54
a, Å	8.555(2)	10.608(2)
b, Å	19.045(2)	18.714(2)
c, Å	19.700(3)	15.404(4)
β, deg	98.59(1)	109.41(1)
Z	4	4
F(000)	1387	1443
V, Å³	3173.7(9)	2884.2(1)
d_{calc}, g/cm³	1.403	1.678
cryst size, mm	0.15 × 0.15 × 0.45	0.13 × 0.35 × 0.35
μ, mm⁻¹	0.64	5.17
no. of unique rflns	4397	4006
no. of rflns with $I > 2\sigma$	3613	3373
no. of variables	340	286
R, R_w	0.028, 0.037	0.037, 0.048
GOF	1.33	1.58
max shift/σ	0.022	0.031
res electron density, e/Å³	0.32	1.54

Table 4. Final Atomic Coordinates and Equivalent Isotropic Displacement Ceofficients for Compound 3

	x	y	z	B_{eq},[a] Å²
Mo	0.70831(3)	0.22677(1)	0.03282(1)	2.409(1)
P1	0.86702(10)	0.33638(4)	0.00978(4)	2.54(3)
P2	0.94790(12)	0.40141(4)	0.19474(4)	3.27(4)
P3	0.85926(10)	0.19905(4)	0.15242(4)	2.73(3)
S	1.10363(15)	0.47386(5)	0.18788(5)	5.48(5)
N1	0.8582(4)	0.4039(1)	0.0651(1)	3.33(13)
N2	0.7971(3)	0.4039(1)	0.0651(1)	3.33(13)
N2	0.7971(3)	0.4003(1)	0.1284(1)	3.02(12)
N3	1.0239(3)	0.3192(1)	0.190(7)	3.10(11)
N4	0.9156(3)	0.2671(1)	0.2073(1)	2.97(11)
O1	0.4917(3)	0.2355(1)	−0.1094(1)	5.08(13)
O2	0.4605(3)	0.3206(2)	0.0965(2)	5.22(14)
O3	0.4875(3)	0.1005(1)	0.0547(1)	4.08(13)
O4	0.8745(4)	0.1150(2)	−0.0509(2)	7.32(18)
C1	0.5727(4)	0.2356(2)	−0.0572(2)	3.33(15)
C2	0.5573(4)	0.2897(2)	0.0753(2)	3.35(15)
C3	0.5715(4)	0.1466(2)	0.0483(2)	3.21(14)
C4	0.8283(4)	0.1569(2)	−0.0176(2)	4.19(17)
C5	1.0845(4)	0.3305(2)	0.0084(2)	3.45(15)
C6	1.1340(5)	0.2731(2)	−0.0377(2)	5.05(21)
C7	1.1619(5)	0.4004(2)	−0.0061(2)	5.25(20)
C8	0.7945(4)	0.3855(2)	−0.0702(2)	3.17(14)
C9	0.6272(5)	0.4131(2)	−0.0705(2)	4.36(17)
C10	0.8078(5)	0.3440(2)	−0.1363(2)	4.50(18)
C11	0.6759(5)	0.4552(2)	0.1287(2)	4.38(18)
C12	0.8565(5)	0.4068(2)	0.2716(2)	3.67(17)
C13	0.7137(5)	0.3740(2)	0.2769(2)	4.21(18)
C14	0.6541(6)	0.3748(2)	0.3391(2)	5.33(21)
C15	0.7366(7)	0.4077(2)	0.3945(2)	5.59(24)
C16	0.8761(7)	0.4404(2)	0.3903(2)	5.67(25)
C17	0.9396(5)	0.4406(2)	0.3285(2)	4.60(19)
C18	1.1869(4)	0.3089(2)	0.2275(2)	4.80(19)
C19	0.7351(4)	0.1515(2)	0.2079(2)	3.61(15)
C20	0.8195(6)	0.1292(2)	0.2786(2)	5.89(21)
C21	0.5831(5)	0.1897(2)	0.2166(2)	4.97(19)
C22	1.0323(4)	0.1387(2)	0.1578(2)	4.20(16)
C23	0.9820(6)	0.0628(2)	0.1388(3)	6.54(25)
C24	1.1511(5)	0.1631(2)	0.1125(2)	5.47(21)

[a] B_{eq} is the mean of the principal axes of the thermal ellipsoid.

---

(20) Majoral, J. P.; Kramer, R, R.; Navoch, J.; Mathias, F. *Tetrahedron* **1976**, *32*, 2633.

Table 5. Final Atomic Coordinates and Equivalent Isotropic Displacement Coefficients for Compound 4

	x	y	z	B_{eq},[a] Å^2
Pt	0.329295(25)	0.795189(15)	0.096126(19)	2.511(16)
Cl1	0.10556(20)	0.80413(11)	0.09250(18)	4.34(11)
Cl2	0.34057(24)	0.91737(13)	0.13316(23)	5.88(14)
P1	0.54279(19)	0.80703(10)	0.10482(14)	2.61(8)
P2	0.68138(17)	0.61155(11)	0.12524(13)	2.64(8)
P3	0.29525(17)	0.67858(10)	0.05850(13)	2.27(8)
S	0.66283(21)	0.55851(13)	0.01366(15)	4.16(10)
N1	0.6133(6)	0.7411(4)	0.0635(4)	2.9(3)
N2	0.7199(6)	0.6985(3)	0.1204(5)	2.9(3)
N3	0.5391(5)	0.6158(3)	0.1545(4)	2.7(3)
N4	0.4261(6)	0.6234(3)	0.0719(4)	2.5(3)
C1	0.6593(7)	0.8176(4)	0.2239(5)	3.2(4)
C2	0.6132(9)	0.7740(5)	0.2915(6)	4.6(5)
C3	0.6800(11)	0.8962(5)	0.2558(7)	5.7(5)
C4	0.5657(8)	0.8837(4)	0.0375(6)	3.8(4)
C5	0.7067(10)	0.8903(6)	0.0325(7)	5.7(5)
C6	0.4624(10)	0.8825(5)	−0.0601(6)	5.4(5)
C7	0.8453(8)	0.7112(5)	0.1002(7)	4.9(6)
C8	0.8114(7)	0.5792(4)	0.2268(5)	3.1(4)
C9	0.8625(9)	0.6223(5)	0.3026(6)	5.3(6)
C10	0.9613(11)	0.5956(7)	0.3799(9)	6.5(6)
C11	1.0068(10)	0.5276(7)	0.3811(8)	6.7(6)
C12	0.9552(10)	0.4847(6)	0.3077(8)	6.7(6)
C13	0.8568(9)	0.5110(5)	0.2270(7)	5.1(5)
C14	0.5221(8)	0.5540(5)	0.2105(6)	4.0(4)
C15	0.1804(6)	0.6386(4)	0.1119(5)	2.7(3)
C16	0.2259(9)	0.6508(5)	0.2159(6)	4.6(5)
C17	0.1466(9)	0.5591(5)	0.0873(7)	4.4(4)
C18	0.2134(7)	0.6609(5)	−0.0657(5)	3.4(4)
C19	0.0785(11)	0.6960(7)	−0.1044(7)	6.9(6)
C20	0.3036(10)	0.6836(6)	−0.1223(6)	5.0(5)

[a] B_{eq} is the mean of the principal axes of the thermal ellipsoid.

crystalline solid in 35% yield. The IR, ^{1}H, and ^{31}P NMR spectra were similar to those of complex **2**.

X-ray Data Collection and Processing. The crystal data and details of data collection for **2** and **3** are listed in Table 3. Yellow crystals of **3** suitable for X-ray diffraction were obtained from CH_2Cl_2/hexane (1:3 v/s) at 0 °C, whereas suitable crystals of **4** were obtained by slow evaporation of its acetonitrile solution. All X-ray data were collected on a Enraf-Nonius CAD-4 diffractometer with Mo Kα radiation and a graphite monochromator at 22(1) °C. The cell dimensions were obtained from a least-squares fit to setting angles of 25 reflections with the 2θ angle in the range 20.0–30.0°. Both the crystals **3** and **4** exhibited no significant decay under X-ray irradiation. Absorption corrections were made for **3** (μ = 5.17 mm^{-1}); the minimum and maximum transmission factors are 0.339 to 0.998.

The structures were solved by direct methods and were subsequently defined by the full-matrix least-squares method which minimizes $\sum w/(|F_o| - |F_c|)^2$, where $w^{-1} = [\sigma(\text{counting}) + (0.008(F_o)^2)/4F_o]$. Atomic scattering factors which included anomalous scattering contributions were from ref 21. All hydrogen atoms in both the structures were located in difference Fourier maps and refined with the fixed isotropic thermal parameters. The final cycle of the least-squares refinement gave an agreement factor R of 0.038 for **3** and 0.037 for **4**. The final positional parameters and their equivalent thermal parameters for all non-hydrogen atoms are listed in Tables 4 and 5, respectively. The programs used for the crystallographic computations are reported in ref 22. Listing of full experimental details, coordinates, temperature factors, and anisotropic temperature factors are deposited as supplementary material.

Acknowledgment. This work was supported by funds provided by DOE Grant DEFG0289E R60875 and by the Departments of Chemistry, Radiology, and Research Reactor, University of Missouri. Partial funding of the X-ray diffractometer by the National Science Foundation, Grant No. CHE[90-11804], is gratefully acknowledged.

Supplementary Material Available: Tables of experimental details, bond distances and angles, atom coordinates, and thermal parameters for **3** and **4** and an ORTEP drawing (7 pages). Ordering information is given on any current masthead page.

OM930844+

---

(21) *International Tables For X-ray Crystallography*; Kynoch Press: Birmingham, U.K., 1974; Vol. 4.

(22) The following references are relevant to the NRCVAX system: (a) Gabe, E. J.; Page, Y. L.; Charland, J. L.; Lee, F. L.; White, P. S. *J. Appl. Crystallogr.* **1989**, *22*, 384. (b) Flack, L. *Acta Crystallogr. Sect. A* **1983**, *39*, 876. (c) Johnson, C. K. *ORTEP—A Fortran Thermal Ellipsoid Plot Program*; Technical Report ORNL-5138; Oak Ridge National Laboratory: Oak Ridge, TN, 1976. (d) Larson, A. C. *Crystallographic Computing*; Munksgaard, Copenhagen, 1970; p 293. (e) Page, Y. L. *J. Appl. Crystallogr.* **1988**, *21*, 983. (f) Page, Y. L.; Gabe, E. J. *J. Appl. Crystallogr.* **1979**, *12*, 464. (g) Rogers, D. *Acta Crystallogr., Sect. A* **1981**, *37*, 7.